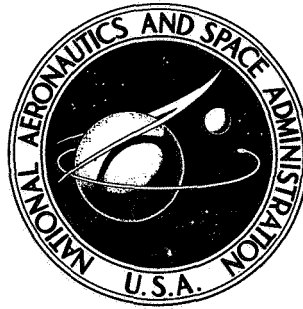


75N15607

**NASA TECHNICAL NOTE**



**NASA TN D-7796**

**NASA TN D-7796**

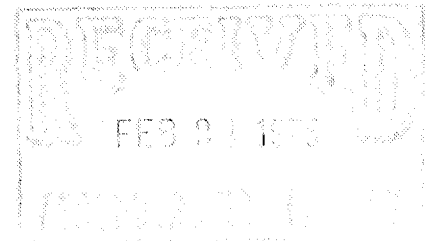
**AN ANALYTICAL EVALUATION  
OF AIRFOIL SECTIONS FOR  
HELICOPTER ROTOR APPLICATIONS**

*Gene J. Bingham*

*Langley Directorate*

*U.S. Army Air Mobility R&D Laboratory*

*Hampton, Va. 23665*



1. Report No. NASA TN D-7796	2. Government Accession No.	3. Recipient's Catalog No.	
4. Title and Subtitle AN ANALYTICAL EVALUATION OF AIRFOIL SECTIONS FOR HELICOPTER ROTOR APPLICATIONS		5. Report Date February 1975	
		6. Performing Organization Code	
7. Author(s) Gene J. Bingham, Langley Directorate, U.S. Army Air Mobility R&D Laboratory		8. Performing Organization Report No. L-9710	
		10. Work Unit No. 501-06-05-07	
9. Performing Organization Name and Address NASA Langley Research Center Hampton, Va. 23665		11. Contract or Grant No.	
		13. Type of Report and Period Covered Technical Note	
12. Sponsoring Agency Name and Address National Aeronautics and Space Administration Washington, D.C. 20546		14. Sponsoring Agency Code	
		15. Supplementary Notes	
16. Abstract  An analytical technique was used to evaluate airfoils for helicopter rotor application. This technique permits assessment of the influences of airfoil geometric variations on drag divergence Mach number at lift coefficients from near zero to near maximum lift. Analytical results presented in this paper indicate the compromises in drag divergence Mach number which result from changes in (1) thickness ratio, (2) location of maximum thickness, (3) leading-edge radius, (4) camber addition, and (5) location of maximum camber for NACA four- and five-digit-series airfoils and some 6-series airfoils of potential interest for helicopters. Examples of airfoil sections which combine several of the geometric changes favorable to both advancing and retreating section performance have been presented.			
17. Key Words (Suggested by Author(s)) NACA airfoils Airfoil design Helicopter airfoils		18. Distribution Statement Unclassified - Unlimited  STAR Category 01	
19. Security Classif. (of this report) Unclassified	20. Security Classif. (of this page) Unclassified	21. No. of Pages 24	22. Price* \$3.25

# AN ANALYTICAL EVALUATION OF AIRFOIL SECTIONS FOR HELICOPTER ROTOR APPLICATIONS

By Gene J. Bingham  
Langley Directorate, U.S. Army Air Mobility R&D Laboratory

## SUMMARY

An analytical technique was used to evaluate airfoils for helicopter rotor application. This technique permits assessment of the influences of airfoil geometric variations on the drag divergence Mach number at lift coefficients from near zero to near maximum lift. Analytical results presented in this paper indicate the compromises in drag divergence Mach number which result from changes in (1) thickness ratio, (2) location of maximum thickness, (3) leading-edge radius, (4) camber addition, and (5) location of maximum camber for NACA four- and five-digit-series airfoils and some six-series airfoils of potential interest for helicopters.

Examples of airfoil sections which combine several of the geometric changes favorable to both advancing and retreating section performance have been presented. These sections had thicknesses from 8 to 12 percent chord with maximum thickness at 40 percent chord, standard NACA four- and five-digit-series airfoil leading-edge radius, and maximum camber at 35 percent chord. The 12-percent-thick section had a higher drag divergence Mach number than the classic NACA 0012 airfoil at lift coefficients greater than zero. The thinner sections provided even higher drag divergence at lift coefficients below 1.0. Although the final selection of an airfoil, or combination of airfoils, for a helicopter rotor should be made on the basis of the specific performance requirements, the methods of analysis employed in this investigation can be rapidly and effectively used with high confidence during preliminary airfoil selection.

## INTRODUCTION

The NACA 0012 airfoil section was used almost exclusively on operational helicopters from 1939 to about 1965. Other airfoils were hardly considered during this period because aerodynamic problems were secondary to the many mechanical and structural problems that had to be solved. About 1965, aerodynamic considerations resulted in the use of the NACA 23012 airfoil on one operational helicopter. Since then, several programs have been conducted to improve the aerodynamic characteristics of airfoils for helicopter rotors and to define a systematic approach to rotor airfoil design and selection (refs. 1 to 6).

As part of the continuing effort, an analytical investigation was initiated to define the lift coefficients and Mach numbers for airfoils of potential interest for helicopter application. The primary objective was to determine the effects of changes in airfoil geometric parameters such as thickness, thickness distribution, leading-edge radius, camber, and camber distribution on lift—Mach-number characteristics.

The analysis was based on the drag divergence Mach number prediction techniques of references 7 and 8. The airfoils considered were from the NACA four-digit-, five-digit-, and 6-series families reported in reference 9 and are generally consistent with the pitching-moment coefficient criterion suggested by reference 6. The airfoil coordinates were derived by applying references 10, 11, and 12.

### SYMBOLS

$C_p$	static pressure coefficient, $\frac{p_{\text{local}} - p_{\infty}}{q_{\infty}}$
$C_{p,\text{crest}}$	static pressure coefficient at airfoil crest (chordwise station at which airfoil surface is tangent to free stream)
$c$	chord of airfoil, cm
$c_d$	section drag coefficient
$c_l$	section lift coefficient
$c_{m,\text{ac}}$	section pitching-moment coefficient about aerodynamic center
$M_{\text{cr}}$	critical Mach number of airfoil section, free-stream Mach number at which local sonic velocity is first reached on airfoil surface
$M_d$	drag divergence Mach number, $\frac{dc_d}{dM_{\infty}} = 0.1$
$M_{\infty}$	free-stream Mach number
$p_{\text{local}}$	local static pressure, $\text{N/m}^2$
$p_{\infty}$	free-stream static pressure, $\text{N/m}^2$
$q_{\infty}$	free-stream dynamic pressure, $\text{N/m}^2$

R	rotor blade radius
x	distance measured along airfoil chord, cm
$x_{\text{crest}}$	distance measured along airfoil chord from leading edge to crest, cm
z	distance measured perpendicular to airfoil chord, cm
$\alpha$	angle of attack of airfoil, deg
$\psi$	rotor blade azimuth angle (measured counterclockwise from aft blade position), deg

## ANALYTICAL METHOD

### Background

In several respects, the airfoil section requirements for a helicopter rotor are more complex than those for a fixed-wing aircraft. On a single revolution, the sections can experience lift coefficients from negative values to maximum lift and free-stream Mach numbers from low subsonic to transonic values (refs. 1 to 6). Representative envelopes of lift coefficient varying with Mach number at 0.611R, 0.806R, and 1.0R (the rotor tip) and a flight velocity of 136 knots for a vehicle weight of 2700 kg are shown in figure 1(a) (ref. 5). At the rotor tip, the airfoil section advancing into the wind operates at a Mach number near 0.9 at near zero lift coefficient and the retreating airfoil section operates up to a lift coefficient of 1.4 (near maximum lift) at Mach 0.45.

The drag divergence Mach number  $M_d$  for the airfoil section employed has been superimposed on figure 1(a); the drag divergence Mach number is defined as the free-stream Mach number at which the rate of increase of drag coefficient with Mach number equals 0.1. As noted in the figure, beyond about 0.7R to 0.8R, which includes over one-third of the rotor disk area, the airfoil sections operate at Mach numbers above drag divergence. Of course, the increase in drag has a prime influence on the power required to drive the rotor and, thus, on the maximum lift capability. Therefore, an airfoil is desired which would have the drag divergence Mach number line located at as large a radius station as possible.

Shown in figure 1(b) is the variation of lift coefficient with Mach number calculated for a second rotor at 0.95R and a flight velocity of 150 knots for vehicle weights of 5230 kg and 3420 kg. For the heavier vehicle, the drag divergence Mach number will be exceeded by the advancing blade only at lift coefficients below 0.8; for the lighter weight, below 0.4.

Although not shown in the figure, the drag divergence for these cases extends inboard to about  $0.8R$ . An analysis of this rotor indicates that each increase of about 0.01 in drag divergence Mach number for the complete lift-coefficient range of figure 1(b) would result in a 4-percent power saving for these operating conditions. For this analysis, all parameters except the drag divergence Mach numbers were unchanged. A larger power saving would be expected at higher flight velocities or with the configuration of figure 1(a) because more of the rotor would operate beyond drag divergence.

Because of such potential savings, one objective of the present analysis was to determine how to increase the drag divergence Mach number. More specifically, the intent was to determine the influence of the individual variations in airfoil geometric parameters on drag divergence Mach number, and then to examine them in combination.

### Approach

References 7 and 8 show that drag divergence can be predicted at lift coefficients from zero to near maximum lift if the airfoil static pressure distribution at low subsonic speeds and the location of the airfoil crest are known. The airfoil crest position for a selected airfoil and its variation with angle of attack is illustrated in figure 2. The crest used herein is defined as the chordwise station at which the airfoil surface is tangent to the free stream. Also, representative subsonic static pressure distributions have been plotted for this airfoil, and the crest static pressure coefficient has been identified.

Drag divergence results from changes in the pressure distribution on the airfoil surface caused by increases in Mach number. At free-stream Mach numbers below  $M_{CR}$ , the drag coefficient is generally Mach number independent. (For example, see ref. 13.) At Mach numbers above  $M_{CR}$ , supersonic flow develops in the low-pressure region of the airfoil, and this region contains alternate expansion and compression waves (refs. 7 and 14), which change the surface pressure distribution. If the entire supersonic flow region is ahead of the crest, the change with increases in Mach number can cause the drag coefficient to increase, decrease, or remain constant. Increases, often called the creepy drag rise, result from net increases in pressure force acting on the frontal area ahead of the crest, that is, a drag force. Similarly, decreases observed by several investigators (for example, ref. 13) result from net decreases in pressure force on the frontal area ahead of the crest, that is, a forward suction force. However, if the net pressure force is unchanged, the drag coefficient is insensitive to Mach number increases up to the drag divergence Mach number. As the Mach number is increased sufficiently to cause sonic flow to extend behind the airfoil crest, the observation is made in reference 7 that the expansion and compression waves cause the pressure coefficients ahead of the crest to become less negative and those behind the crest to become more negative, which results in drag divergence. Also, the shock-wave influences on the drag rise can first appear at

a slightly higher Mach number than the drag divergence value; thus, the drag divergence Mach number can be free of the influences of the interaction between the shock wave and the boundary layer. From the discussion in reference 14, it appears that the majority of airfoils experience this type of drag divergence. It is suggested in reference 15 that at the crest, a value of 0.515 for the ratio of local static pressure to free-stream total pressure is more appropriate to predictions of drag divergence than sonic Mach number. The corresponding Mach number for flow free of shock waves is 1.02. This empirical criterion was applied to about 30 airfoils, each at several angles of attack, in reference 16 and it was concluded that the analytical results generally agreed with experimental drag-rise Mach number results within  $\pm 0.015$ . Reference 16 defines the experimental drag-rise Mach number as the value at initial departure from the subcritical  $M_\infty < M_{CR}$  drag coefficient. If the criterion of  $dc_d/dM_\infty = 0.1$  had been used, sonic velocity at the airfoil crest would provide a better correlation of analytical and experimental results than would the pressure ratio of 0.515. With either approach, differences in drag divergence Mach number for various airfoils would be approximately the same; as discussed later, differences or trends resulting from changes in geometric parameters are of prime interest herein. In the present effort, sonic crest velocity has been used to predict drag-rise Mach numbers because this method is believed to have a better foundation, based on the discussion in the previous paragraphs.

The lift coefficients also are influenced by the changes in pressure distribution with increasing Mach number. When supersonic flow develops on the airfoil, the reduced pressure coefficients in the supersonic region cause an increase in the lift coefficient greater than that predicted by the Prandtl-Glauert factor (ref. 13). This increase continues until lift divergence occurs, which is evidenced by a reduction in the lift coefficient with further increases in Mach number at a constant angle of attack. This reduction usually occurs at a Mach number slightly higher than the drag divergence value; that is, the reduced pressure region behind the crest that causes the drag rise can have a favorable influence on lift coefficient.

The variation of pitching-moment coefficient with Mach number is not as clearly understood as the drag and lift coefficients. Data for some airfoils (ref. 17) suggest the pitching-moment coefficient would vary according to the Prandtl-Glauert factor; however, data for others (for example, ref. 13) show different trends.

#### Application

The application of the analytical approach involves several steps: (1) low-speed pressure distributions, lift coefficients, pitching-moment coefficients, and crest location at selected angles of attack were determined by a compressible-viscous-flow mathematical model described in reference 18; (2) the pressure coefficient at the crest was identified;

(3) the Prandtl-Glauert compressibility factor was applied to the crest pressure coefficient to determine the free-stream Mach number at which sonic flow would exist at the airfoil crest (defined as drag divergence Mach number); and (4) the Prandtl-Glauert factor was applied to the computed lift coefficients to predict the lift coefficients at the drag divergence Mach numbers.

At present, the available aerodynamic computational tools do not permit predictions of the maximum lift coefficient because the computed results are not valid for cases with significant boundary-layer separation. In this investigation, results from the mathematical model with separation forward of 98 percent chord (at a selected Reynolds number of  $10 \times 10^6$ ) are excluded. In instances where the maximum lift coefficient at low subsonic Mach numbers could be determined from experimental results (for example, from ref. 9), the application of analytical results was carried to the known maximum lift coefficient.

As previously discussed, the pitching-moment coefficient does not follow that predicted by the Prandtl-Glauert factor. Therefore, because of the absence of an effective prediction criterion, the pitching-moment coefficients predicted by the mathematical model have been employed. Moreover, adequate predictions of drag by mathematical models are not currently available within the state of the art and, therefore, are not used in this analysis. As suggested in reference 6, an allowable pitching-moment coefficient of  $|0.02|$  has been adopted in this analysis.

## RESULTS AND DISCUSSION

The crest location and the static pressure coefficients at the crest of each airfoil discussed are presented in figure 3 as a function of lift coefficient. Then, the influence of the more important independent geometric variables (thickness, thickness distribution, leading-edge radius, camber, and position of maximum camber) on drag divergence Mach numbers at various section lift coefficients have been predicted and are presented in figures 4 to 9. Data are included for NACA four-digit-, five-digit-, and 6-series airfoils to indicate the generality of the results.

### Thickness Variations

The influence of variations in the thickness-chord ratio is presented in figure 4. The airfoils presented are symmetrical sections; the four-digit and five-digit airfoils have the same thickness distribution and, therefore, have the same aerodynamic characteristics. At zero lift coefficient, increasing the thickness-chord ratio from 0.08 to 0.16 decreased the drag divergence Mach number about 0.08 for the four- and five-digit-series airfoils and about 0.10 for the 6-series airfoils. The decrease was caused by an increase in the magnitude of the crest pressure coefficient with increases in thickness (figs. 3(a) and 3(b)). As the maximum indicated lift coefficient was approached, the crest pressure coefficient

trends with increasing thickness reversed which results in a higher drag divergence Mach number for the thicker sections. Then, the crest is farther aft for the thicker sections so that the pressure coefficient is of lower magnitude. The results of reference 9 suggest higher maximum lift coefficients for the NACA four- and five-digit-series airfoils than for the NACA 6-series airfoils of the same thickness ratio. The pitching-moment coefficient about the aerodynamic center of the symmetrical sections is 0.000.

The effects of changes in the location of maximum thickness are presented in figure 5. Results are presented for the four- and five-digit airfoils, with the maximum thickness located from 30 to 50 percent chord as indicated by the last digit of the airfoil designation. The maximum thickness for the 63<sub>1</sub>-012 and 65<sub>1</sub>-012 sections is at 35 and 40 percent chord, respectively. At zero lift coefficient, the drag divergence Mach number for the NACA four- and five-digit-series airfoils is increased about 0.03 by moving the maximum thickness location aft from 30 to 50 percent chord because both the aft movement of the airfoil crest and the accompanying thinning of the leading-edge region resulted in crest pressure coefficients of smaller magnitude (fig. 3(c)). The increase was slightly greater at a lift coefficient of 0.4. At higher lift coefficients, the crest was more aft for the NACA 0012-63 section than for the other two airfoil sections and resulted in a crest static pressure of smaller magnitude and a higher drag divergence Mach number. The crest position of the NACA 65<sub>1</sub>-012 section was farther aft than that of the 63<sub>1</sub>-012 section only at the lower lift coefficients (fig. 3(d)). However, the magnitude of the pressure coefficient of the NACA 65<sub>1</sub>-012 was lower at all lift coefficients analyzed (fig. 5), which resulted in a consistently higher drag divergence Mach number than for the NACA 63<sub>1</sub>-012 section. From this analysis, it appears that at lift coefficients below 1.3, a maximum thickness location of about 40 percent chord is a reasonable compromise with respect to drag divergence Mach number. Again, the absence of camber results in a pitching-moment coefficient of 0.000.

#### Leading-Edge Radius

The influence of variations in leading-edge radius is indicated in figure 6 only for the NACA four- and five-digit airfoils. The 6-series airfoils were excluded because the leading-edge radius is not a design variable. The -33, -63, and -93 sections have leading-edge radii which are one-fourth normal, normal, and three times normal, respectively (ref. 10). At zero lift coefficient, the drag divergence Mach number increased about 0.02 when the leading-edge radius was increased from one-fourth to three times normal. This increase resulted from a decrease in magnitude of the static pressure coefficient at the crest (figs. 3(e) and (f)); the crest location at zero lift was the same for all three sections. At lift coefficients approaching the maximum, the crest of these four- and five-digit-series airfoils moved rapidly forward as the leading-edge radius was increased, and the pressure

coefficient increased in magnitude to result in a decrease in drag divergence Mach number. An increase in leading-edge radius from one-fourth to normal had little influence on drag divergence for the NACA 23012 airfoil.

### Camber

The effects of camber (figs. 7, 8, and 9) were investigated only on the NACA five-digit and 6-series airfoils because the type of camber for the NACA four-digit airfoils produces excessive pitching moment for helicopter rotor application. The camber addition to the airfoils, shown in figure 7, is proportional to the design lift coefficients of 0.0, 0.3, and 0.6 for the NACA 0012-63, 23012-63, and 43012-63 airfoils and to the design lift coefficients of 0.0, 0.2, and 0.5 for the NACA 63<sub>1</sub>-012; 63<sub>1</sub>-212,  $\alpha = 0.0$ ; and 63<sub>1</sub>-512,  $\alpha = 0.0$  airfoils, respectively (ref. 9). The camber addition caused a decrease in drag divergence Mach number as great as 0.02 at zero lift coefficient because the magnitude of the crest pressure coefficient increased. At lift coefficients above about 0.6 for the five-digit airfoils (fig. 3(g)) and for all lift coefficients for the 6-series airfoils (fig. 3(h)), the crest location was moved aft by the addition of camber.

At high lift coefficients, the favorable influence of increased camber resulted from smaller pressure coefficients at the crest. (See fig. 7.) Although the pitching-moment coefficient of the NACA 63<sub>1</sub>-512,  $\alpha = 0.0$  airfoil exceeded the  $|0.02|$  criterion of reference 6 by a factor of 2, the results have been included to discern the trends. To satisfy this criterion, the maximum design lift coefficient should be 0.25 instead of 0.5 because within the linear theory, pitching-moment coefficient is proportional to design lift coefficient (ref. 9). Also, observe that the NACA five-digit airfoils permit a higher design lift coefficient than the NACA 6-series airfoils without exceeding the  $|0.02|$  pitching-moment criterion.

The effect of varying the location of maximum camber is presented in figure 8. The maximum camber is at 5, 15, and 25 percent chord for the 21012-63, 23012-63, and 25012-63 airfoils, respectively, and at 32.5 and 50 percent chord for the 63<sub>1</sub>-212,  $\alpha = 0.0$  and 63<sub>1</sub>-212,  $\alpha = 1.0$  airfoils, respectively. These locations represent the limits defined for the standard NACA five-digit- and 6-series airfoils (ref. 9). At near zero lift coefficient, the results show that the position of maximum camber (figs. 3(i) and 3(j)) has little influence on drag divergence Mach number (fig. 8). The most significant influence is at high lift coefficients for the five-digit sections. At these conditions, the most rearward position of maximum camber resulted in the most rearward crest locations and the lowest magnitudes of pressure coefficient and, thus, the highest drag divergence Mach numbers. The aft movement of maximum camber also increased the pitching-moment coefficient, but it does meet the  $|0.02|$  criterion of reference 6 for the NACA five-digit-series airfoils

presented. The pitching-moment coefficient of the NACA 63<sub>1</sub>-212,  $a = 1.0$  airfoil is excessive.

In addition to the conventional camber lines, the NACA five-digit airfoil series has been provided with a camber line which has trailing-edge reflex (ref. 11). This reflex permits near zero pitching-moment coefficient at all lift coefficients up to the maximum lift coefficient. At a given lift coefficient, the reflex camber unloads the airfoil trailing-edge region and, hence, increases the magnitude of the forward upper-surface pressure coefficients (fig. 3(k)) compared with those for the conventional camber lines. This forward loading resulted in a corresponding decrease in the drag divergence Mach number at all lift coefficients, as shown in figure 9 where the results for an airfoil with reflex camber (NACA 25112-63) are compared with those for an airfoil without reflex camber (NACA 25012-63). The decrease in drag divergence Mach number varied from 0.025 at zero lift to 0.01 at high lift coefficients.

### Combined Geometry

The influence of combining several of the favorable geometric parameters previously discussed is shown in figures 3(l) and 10. The thickness distribution of the NACA four- and five-digit airfoils has been selected to take advantage of the maximum lift capability at low speeds for the low pitching-moment designs noted previously. The influence of thickness from 8 to 12 percent chord for these cambered sections is presented. Maximum thickness was located at 40 percent chord because, as previously discussed, this position was believed to be a reasonable compromise at lift coefficients below 1.3 (fig. 5). The standard leading-edge radius was selected because it was near optimum for the NACA five-digit airfoils (fig. 6). Camber was added to increase the drag divergence at the higher lift coefficients (fig. 7); however, the camber was limited to satisfy the maximum pitching-moment criterion of  $|0.02|$ . The maximum camber was located at 35 percent chord because of the favorable trends with the aft maximum camber location (fig. 8). The location of maximum camber at 35 percent chord is more aft than that provided by the standard NACA five-digit airfoils. The camber line employed was obtained from reference 19 and was apparently generated by extrapolating the NACA camber-line geometry. The results obtained with these sections are compared with the classic NACA 0012 section in figure 10.

The 12-percent-thick combined-geometry airfoil section has a higher drag divergence Mach number than the 0012 airfoil at all lift coefficients greater than zero. For these configurations, increases in drag divergence Mach number at zero lift can be obtained by decreasing airfoil thickness. As discussed previously and as shown in figure 10, this will result in decreases in drag divergence Mach number at the higher lift

coefficients indicated. The final choice of an airfoil section for a given helicopter rotor should depend on an analysis of the airfoil section requirements.

## CONCLUSIONS

An analytical technique has been used to evaluate airfoils for helicopter rotor application. This technique permits assessment of the influences of airfoil geometric variations on the drag divergence Mach number at lift coefficients from near zero to near maximum lift. Analytical results presented in this paper indicated the compromises in drag divergence Mach number which result from changes in (1) thickness ratio, (2) location of maximum thickness, (3) leading-edge radius, (4) camber addition, and (5) location of maximum camber for NACA four- and five-digit-series airfoils and some 6-series airfoils of potential interest for helicopters.

The results of the airfoil analysis indicated the following conclusions:

1. At zero lift coefficient, increasing the thickness-chord ratio from 0.08 to 0.16 decreased the drag divergence Mach number about 0.08 to 0.10. As the maximum lift coefficient was approached, the trends with increasing thickness reversed.
2. At zero lift coefficient, the drag divergence Mach number increased about 0.03 by moving the maximum thickness location aft from 30 to 50 percent chord. At lift coefficients approaching maximum, the trend reversed. It appears that a maximum thickness location of about 40 percent chord is a reasonable compromise with respect to drag divergence Mach number.
3. At zero lift coefficient, the drag divergence Mach number increased about 0.02 when the leading-edge radius was increased from one-fourth to three times normal. At lift coefficients approaching maximum, the results indicated a decrease in drag divergence Mach number.
4. The camber addition caused a decrease in drag divergence Mach number as great as 0.02 at zero lift coefficient. A favorable influence of increased camber was observed at the higher lift coefficients.
5. At near zero lift coefficient, the results show that the position of maximum camber had little influence on drag divergence Mach number. At high lift coefficients, the most rearward position of maximum camber resulted in the highest drag divergence Mach numbers.
6. A comparison of results for airfoils with conventional camber and with reflex camber for zero pitching moment indicated that the reflex camber caused a general decrease in drag divergence Mach number.

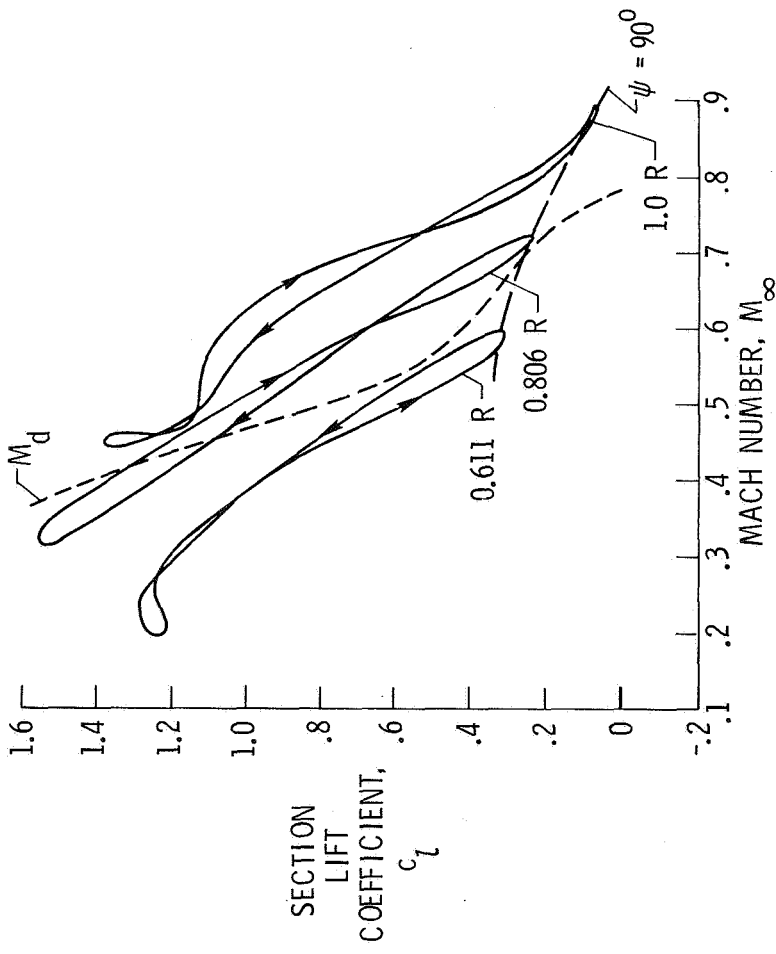
7. By combining several of the favorable geometric parameters, a 12-percent-thick airfoil section was defined which displayed a higher drag divergence Mach number than the 0012-63 airfoil at all lift coefficients greater than zero. Increases in drag divergence Mach number at zero lift were obtained by decreasing airfoil thickness; however, as before, the drag divergence Mach number at the highest lift coefficients investigated was compromised.

Langley Research Center,  
National Aeronautics and Space Administration,  
Hampton, Va., December 2, 1974.

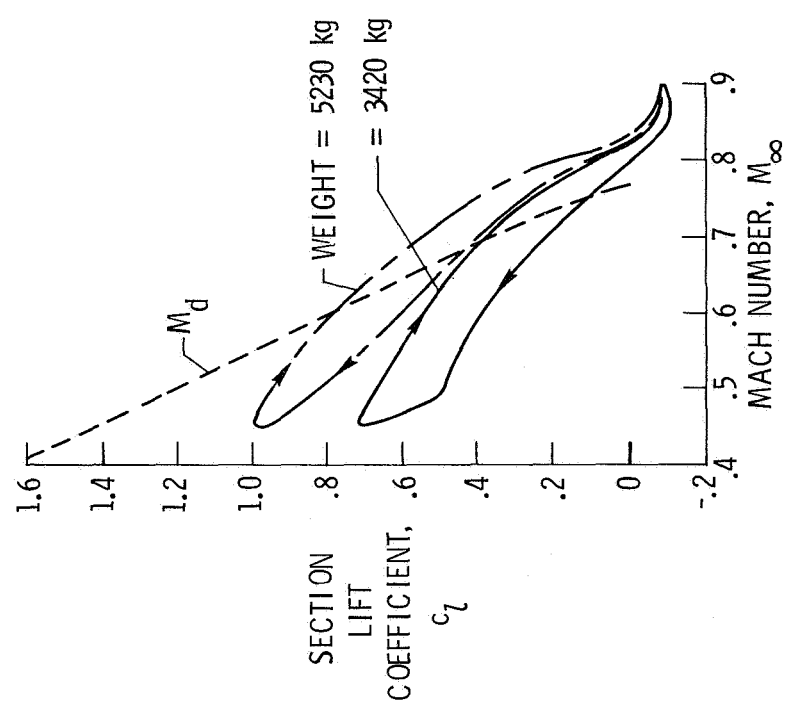
## REFERENCES

1. Davenport, Franklyn J.; and Front, John V.: Airfoil Sections for Helicopter Rotors – A Reconsideration. Proceedings of the Twenty-Second Annual National Forum, American Helicopter Soc., Inc., May 1966, pp. 29-44.
2. Wortmann, F. X.; and Drees, Jan M.: Design of Airfoils for Rotors. CAL/AVLABS Symposium Proceedings: Aerodynamics of Rotary Wing and V/STOL Aircraft, Vol. I – Rotor/Propeller Aerodynamics; Rotor Noise, June 18-20, 1969.
3. Benson, R. Geoffrey; Dadone, Leone U.; Gormont, Ronald E.; and Kohler, Gary R.: Influence of Airfoils on Stall Flutter Boundaries of Articulated Helicopter Rotors. Preprint No. 621, 28th Annual National Forum Proceedings, American Helicopter Soc., Inc., May 1972.
4. Pearcey, H. H.; Wilby P. G.; Piley, M. J.; and Brotherhood, P.: The Derivation and Verification of a New Rotor Profile on the Basis of Flow Phenomena; Aerofoil Research and Flight Test. Aerodynamics of Rotary Wings, AGARD-CP-111, Feb. 1973, pp. 16-1 – 16-18.
5. Reichert, G.; and Wagner, S. N.: Some Aspects of the Design of Rotor Airfoil Shapes. Aerodynamics of Rotary Wings, AGARD-CP-111, Feb. 1973, pp. 14-1 – 14-22.
6. Kemp, Larry D.: An Analytical Study for the Design of Advanced Rotor Airfoils. NASA CR-112297, 1973.
7. Nitzberg, Gerald E.; and Crandall, Stewart M.: A Study of Flow Changes Associated With Airfoil Section Drag Rise at Supercritical Speeds. NACA TN 1813, 1949.
8. Nitzberg, Gerald E.; Crandall, Stewart M.; and Polentz, Perry P.: A Preliminary Investigation of the Usefulness of Camber in Obtaining Favorable Airfoil-Section Drag Characteristics at Supercritical Speeds. NACA RM A9G20, 1949.
9. Abbott, Ira H.; Von Doenhoff, Albert E.; and Stivers, Louis S., Jr.: Summary of Airfoil Data. NACA Rep. 824, 1945.
10. Stack, John; and Von Doenhoff, Albert E.: Tests of 16 Related Airfoils at High Speeds. NACA Rep. 492, 1934.
11. Jacobs, Eastman N.; and Pinkerton, Robert M.: Tests in the Variable-Density Wind Tunnel of Related Airfoils Having the Maximum Camber Unusually Far Forward. NACA Rep. 537, 1935.
12. Ladson, Charles L.; and Brooks, Cuyler W., Jr.: Development of a Computer Program To Obtain Ordinates for NACA 6- and 6A-Series Airfoils. NASA TM X-3069, 1974.

13. Graham, Donald, J.; Nitzberg, Gerald E.; and Olson, Robert N.: A Systematic Investigation of Pressure Distributions at High Speeds Over Five Representative NACA Low-Drag and Conventional Airfoil Sections. NACA Rep. 832, 1945.
14. Pearcey, H. H.: The Aerodynamic Design of Section Shapes for Swept Wings. Advances in Aeronautical Sciences, Vol. 3, Pergamon Press, Inc., c.1962, pp. 277-322.
15. Sinnott, C. S.: Theoretical Prediction of the Transonic Characteristics of Airfoils. J. Aerosp. Sci., vol. 29, no. 3, Mar. 1962, pp. 275-283.
16. Anon.: A Method of Estimating Drag-Rise Mach Number for Two-Dimensional Aerofoil Sections. Transonic Data Mem. 6407, Roy. Aeronaut. Soc., July 1964.
17. Van Dyke, Milton D.: High-Speed Subsonic Characteristics of 16 NACA 6-Series Airfoil Sections. NACA TN 2670, 1952.
18. Stevens, W. A.; Goradia, S. H.; and Braden, J. A.: Mathematical Model for Two-Dimensional Multi-Component Airfoils in Viscous Flow. NASA CR-1843, 1971.
19. Gothert, B.: High Speed Tests in the DVL High Speed Wind Tunnel (2.7 m $\phi$ ) on Aerofoils of the Same Thickness Distribution With Different Cambers (Series NACA f 35 12 - 0.55 40). Rep. & Transl. No. 400, British M.O.S.(A) Völkenrode, May 1947.



(a) Flight velocity, 136 knots; vehicle weight, 2700 kg. (From ref. 5.)



(b) Calculated variation at 0.95R and flight velocity of 150 knots for vehicle weights of 5230 and 3420 kg.

Figure 1.- Variation of section lift coefficient with Mach number during one blade revolution.

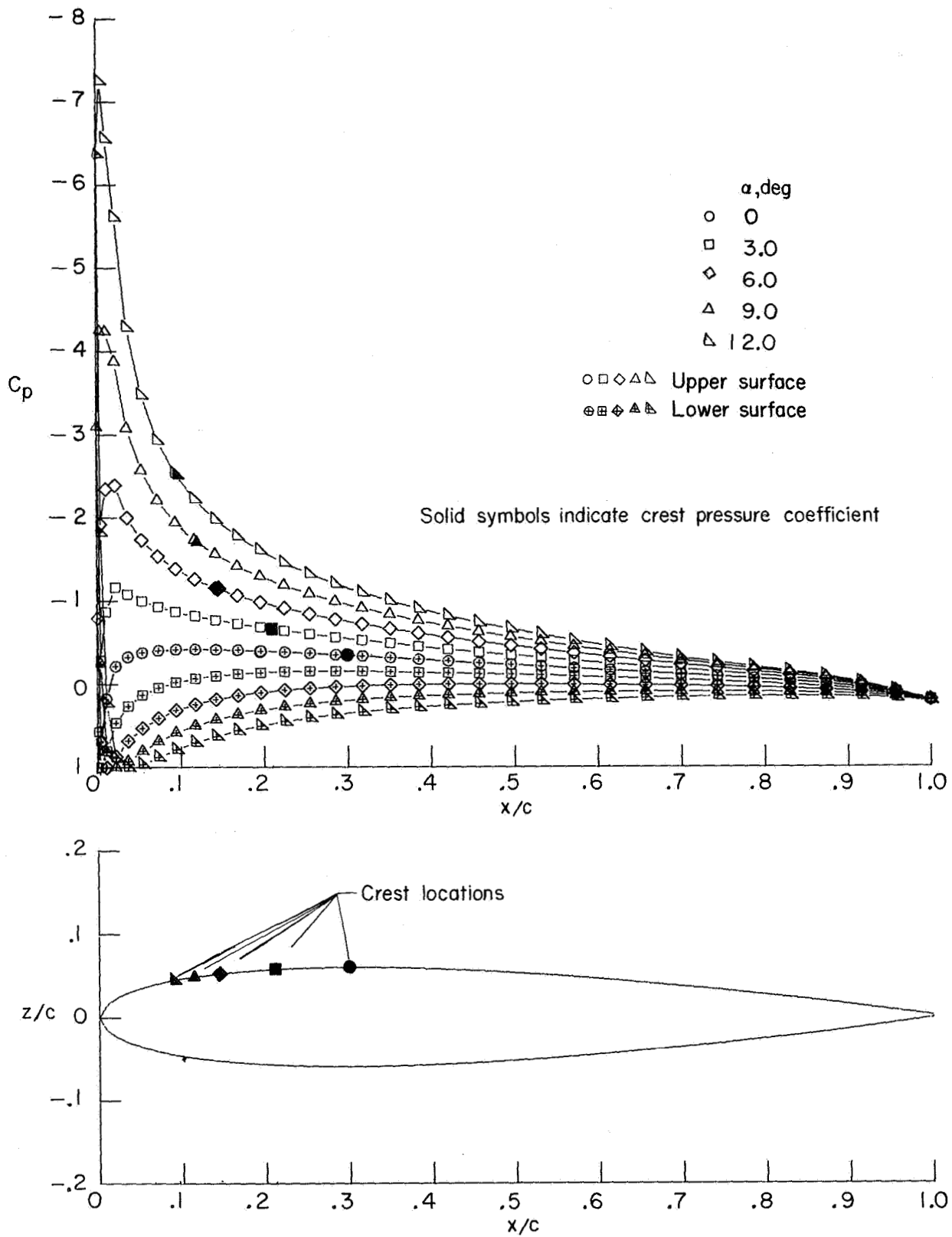
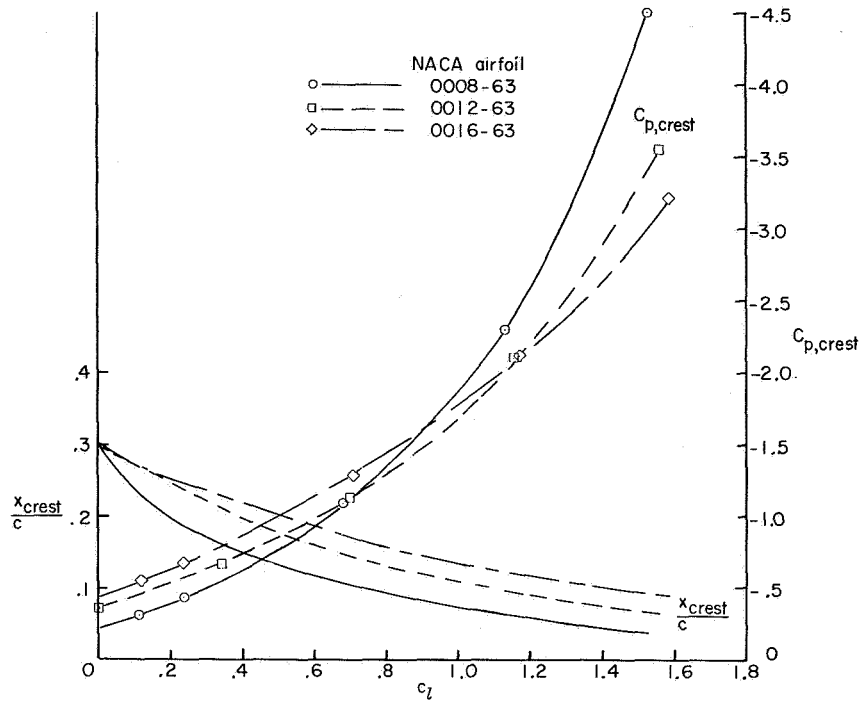
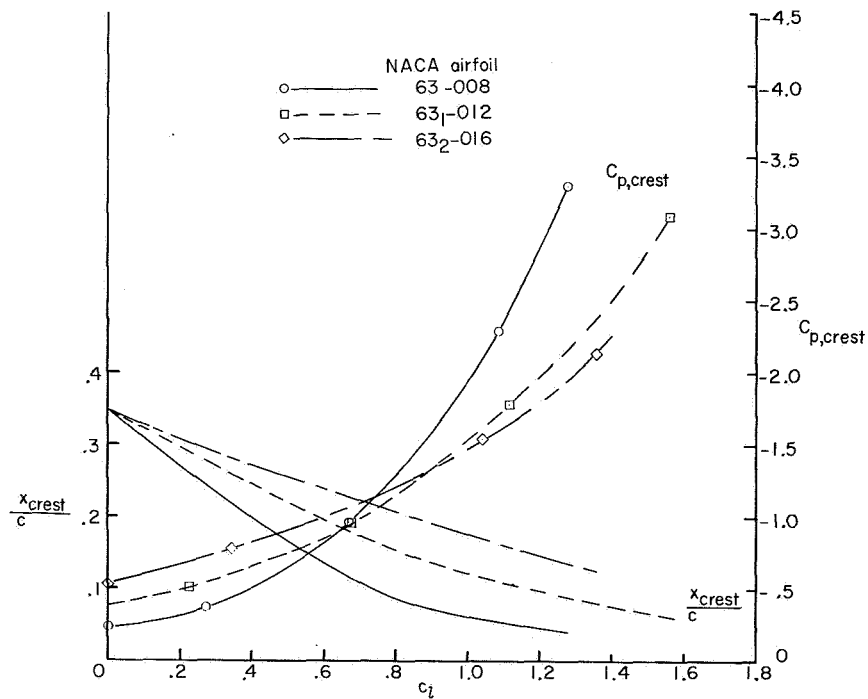


Figure 2.- Typical analytical pressure distribution for NACA 0012-63 airfoil.

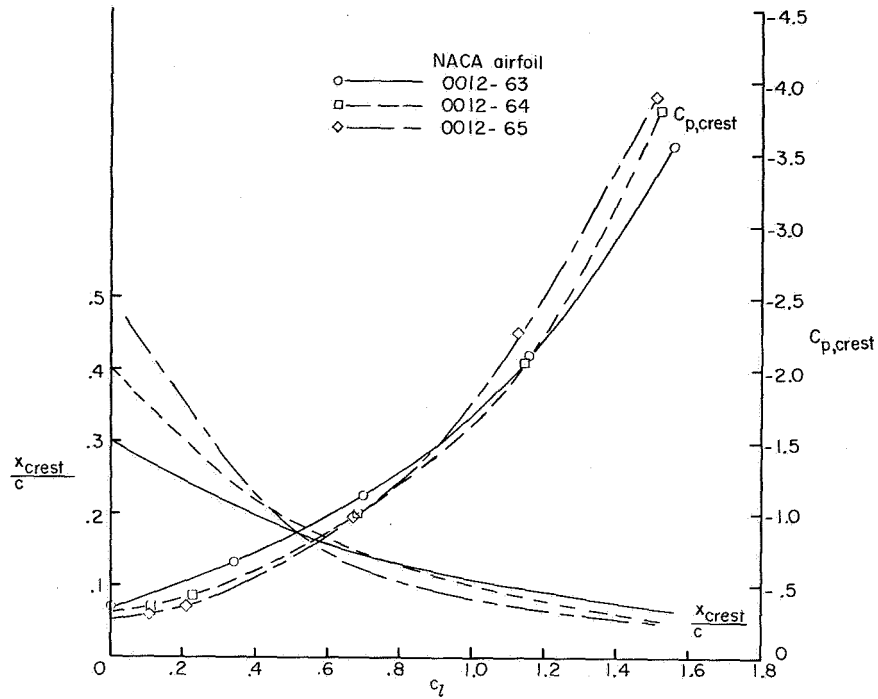


(a) Influence of thickness ratio; four- and five-digit-series airfoils.

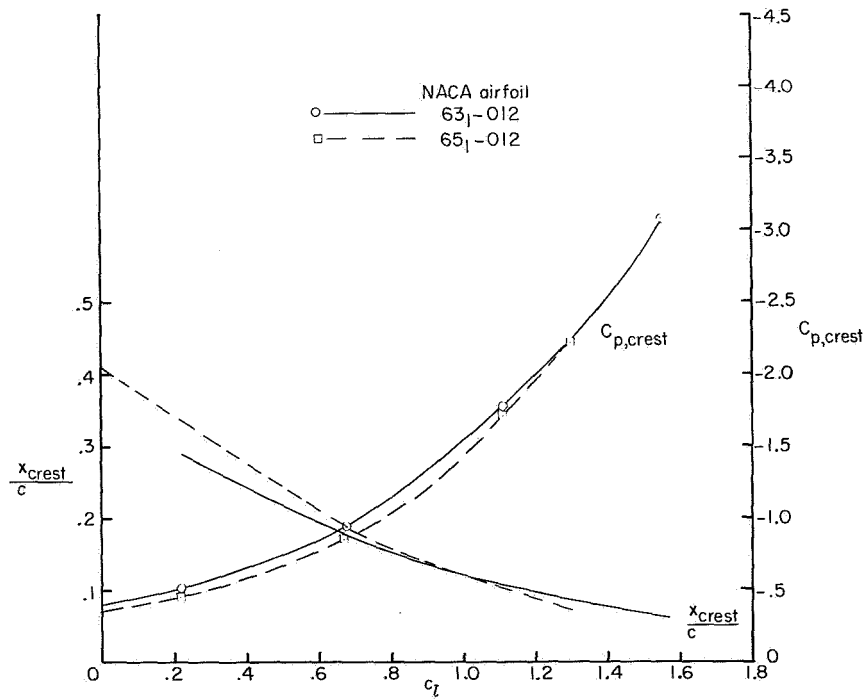


(b) Influence of thickness ratio; 6-series airfoils.

Figure 3.- Variation of crest location and static pressure coefficient at crest ( $M_\infty = 0.20$ ) with section lift coefficient.

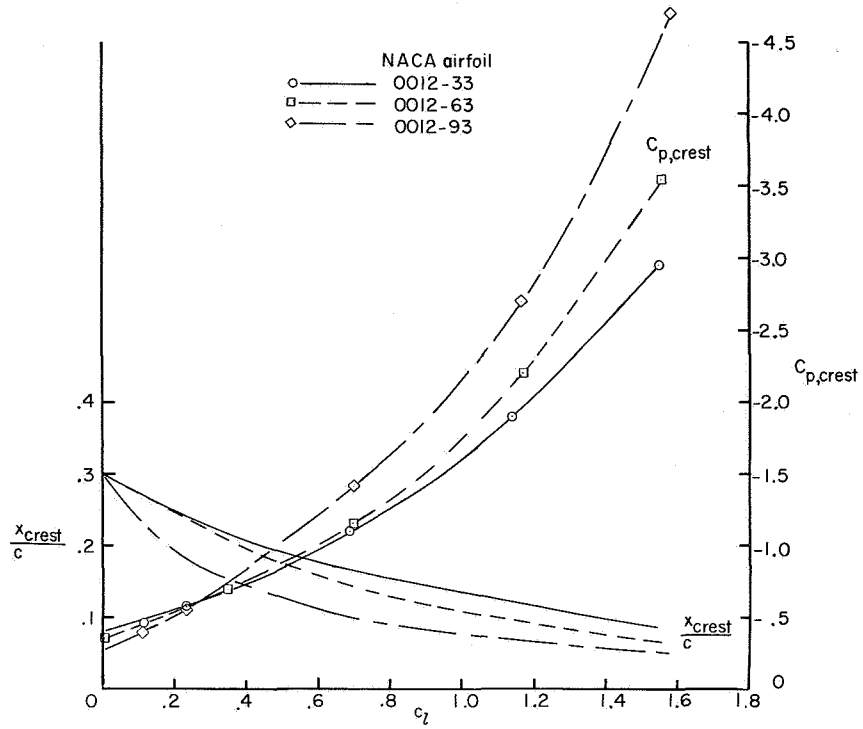


(c) Influence of location of maximum thickness; four- and five-digit-series airfoils.

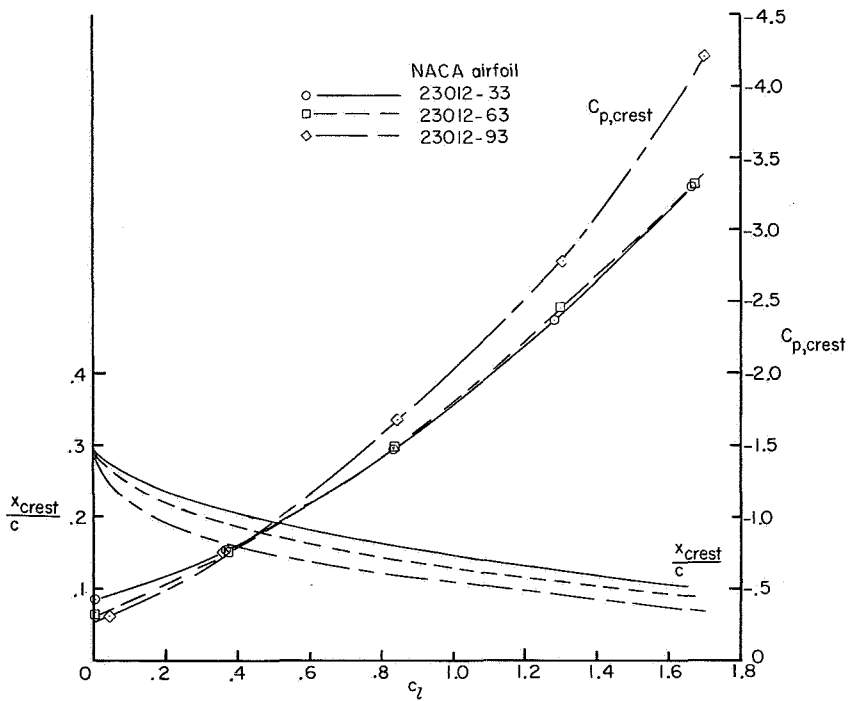


(d) Influence of location of maximum thickness; 6-series airfoils.

Figure 3.- Continued.

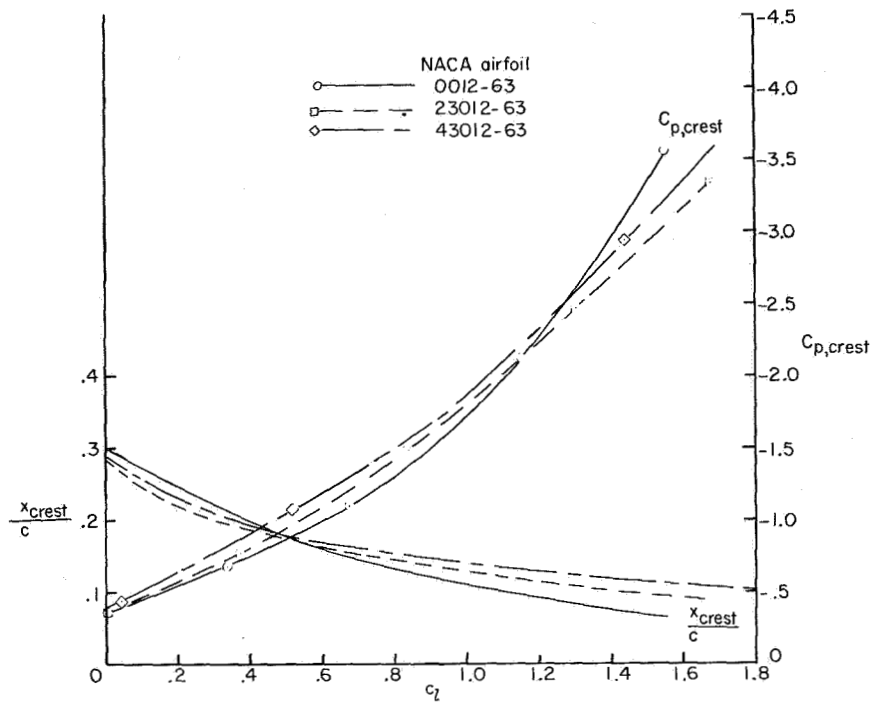


(e) Influence of leading-edge radius; four-digit-series airfoils.

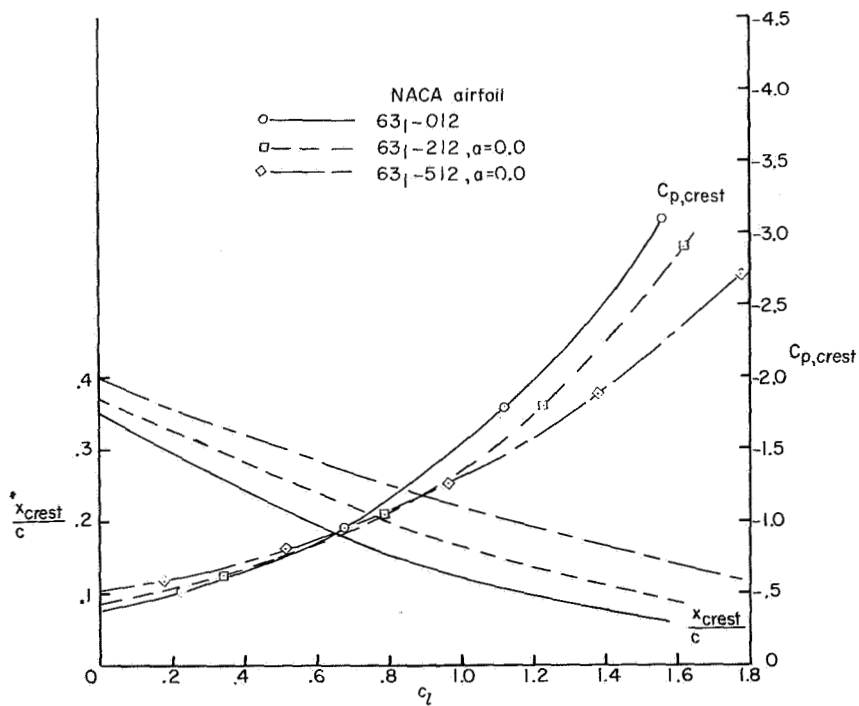


(f) Influence of leading-edge radius; five-digit-series airfoils.

Figure 3.- Continued.

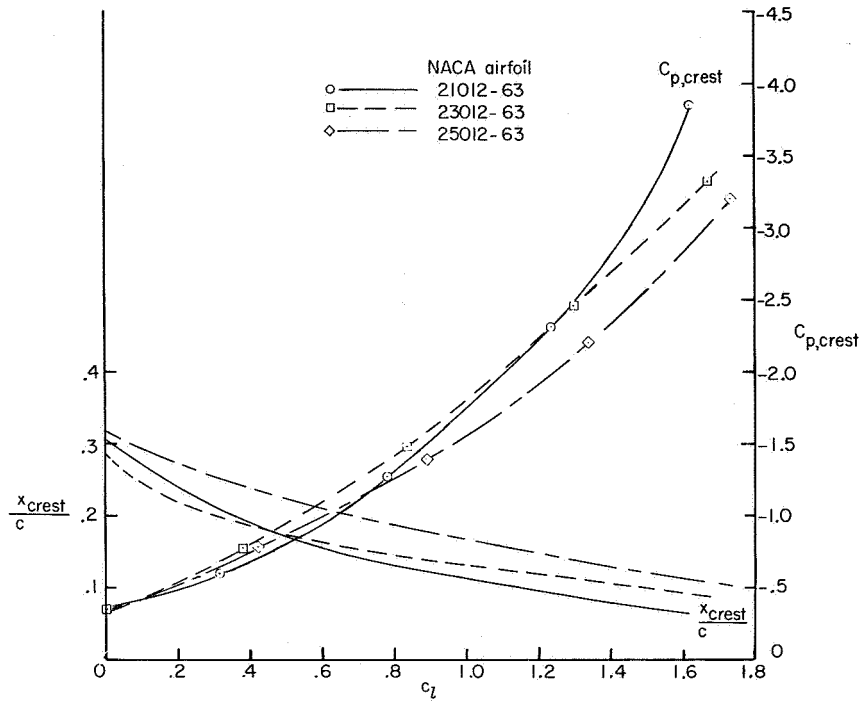


(g) Influence of camber; four- and five-digit-series airfoils.

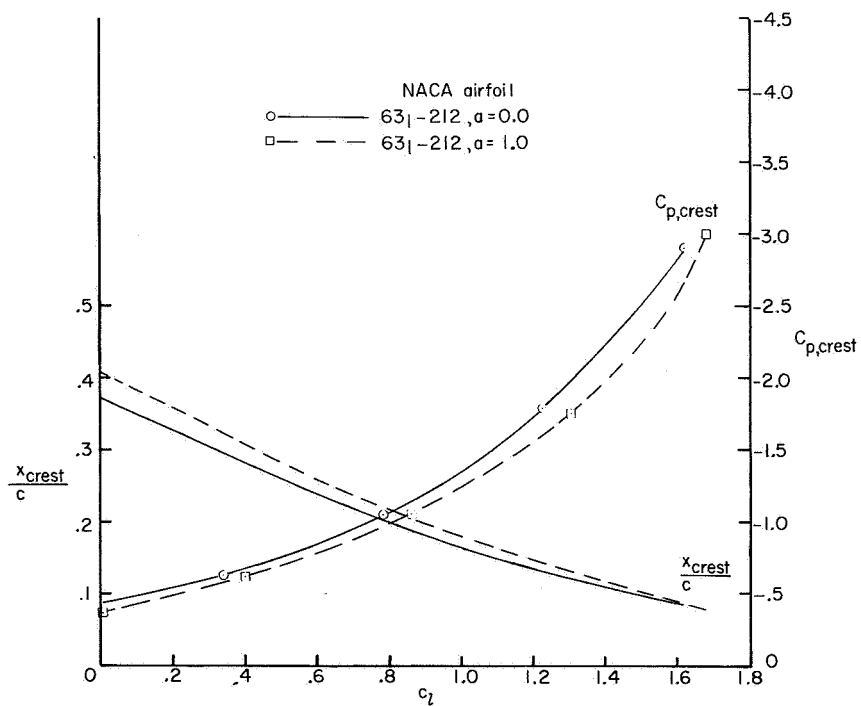


(h) Influence of camber; 6-series airfoils.

Figure 3.- Continued.

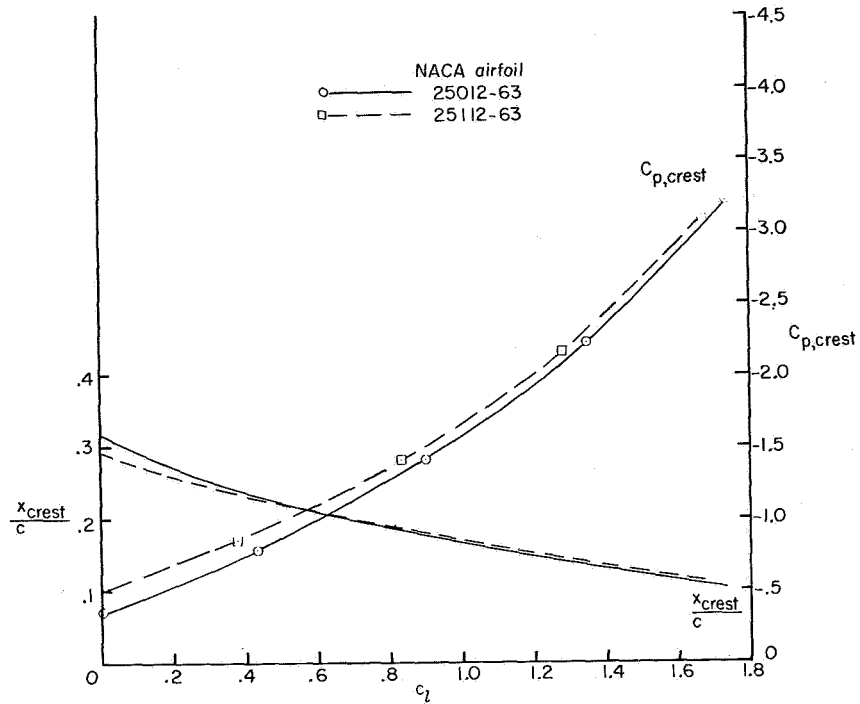


(i) Influence of position of maximum camber; five-digit-series airfoils.

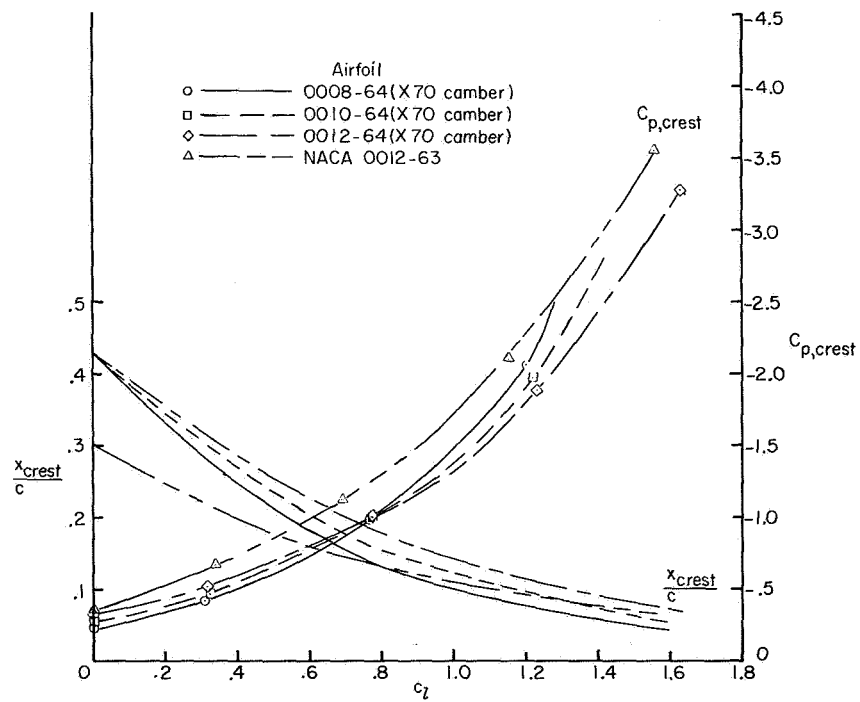


(j) Influence of position of maximum camber; 6-series airfoils.

Figure 3.- Continued.



(k) Influence of reflex camber; five-digit-series airfoils.



(l) Influence of combination of geometric parameters.

Figure 3.- Concluded.

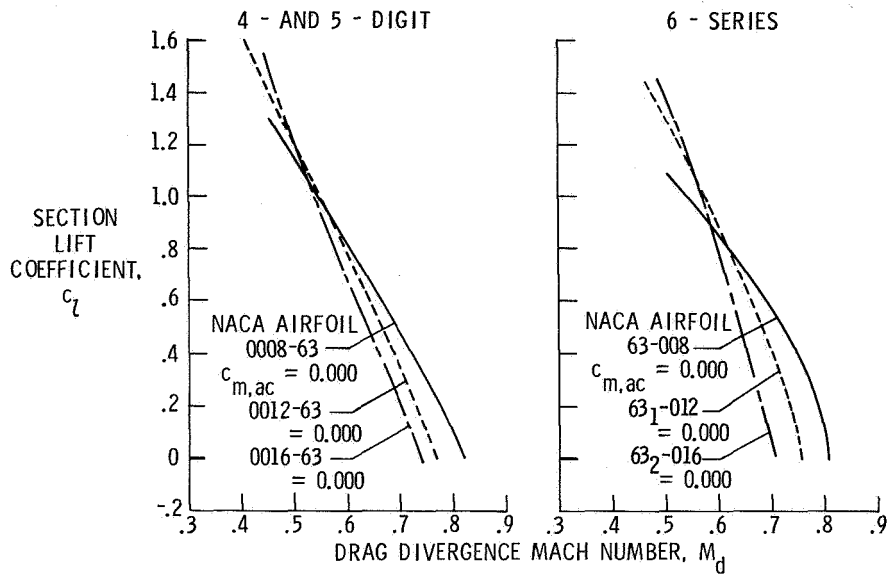


Figure 4.- Influence of thickness-chord ratio on variation of section lift coefficient with drag divergence Mach number.

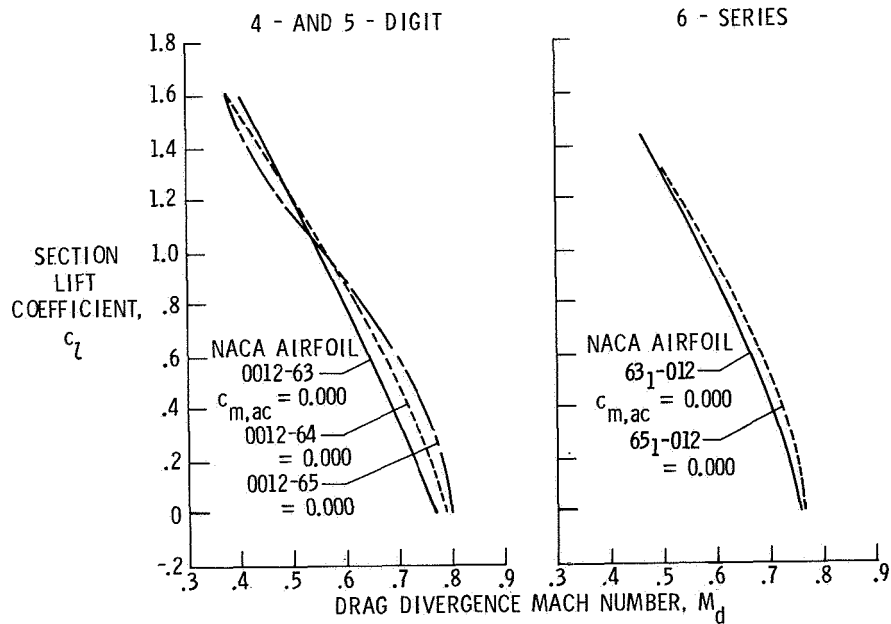


Figure 5.- Influence of maximum thickness location on variation of section lift coefficient with drag divergence Mach number.

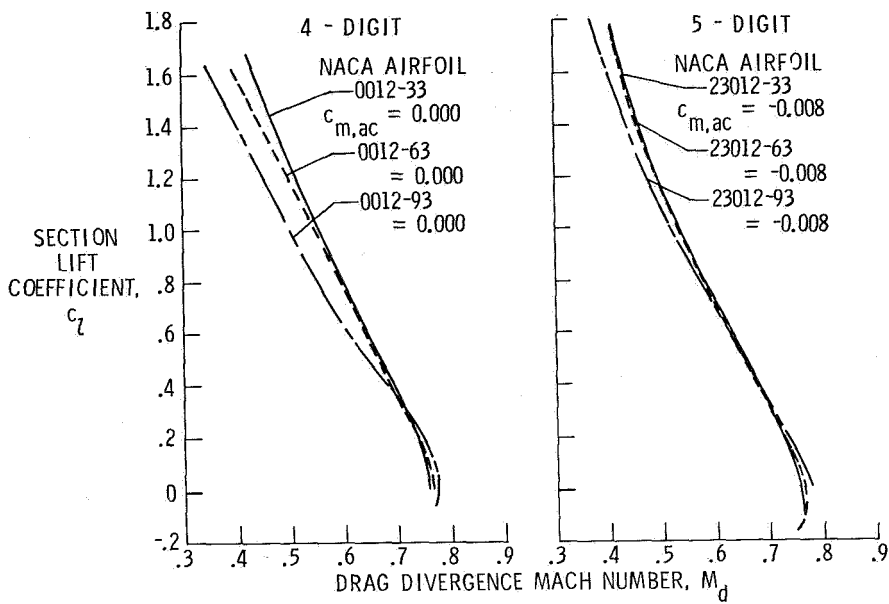


Figure 6.- Influence of leading-edge radius on variation of section lift coefficient with drag divergence Mach number.

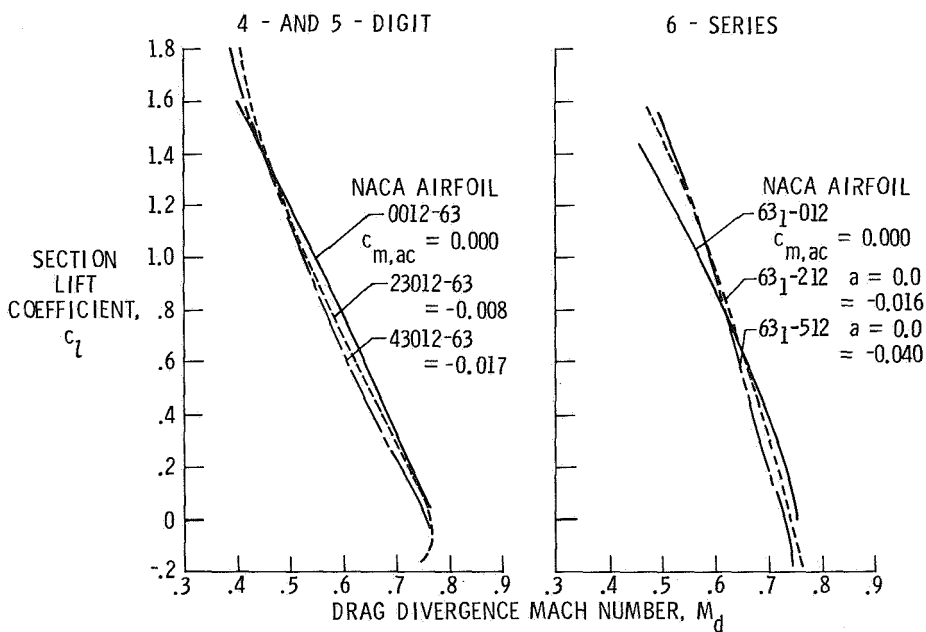


Figure 7.- Influence of camber on variation of section lift coefficient with drag divergence Mach number.

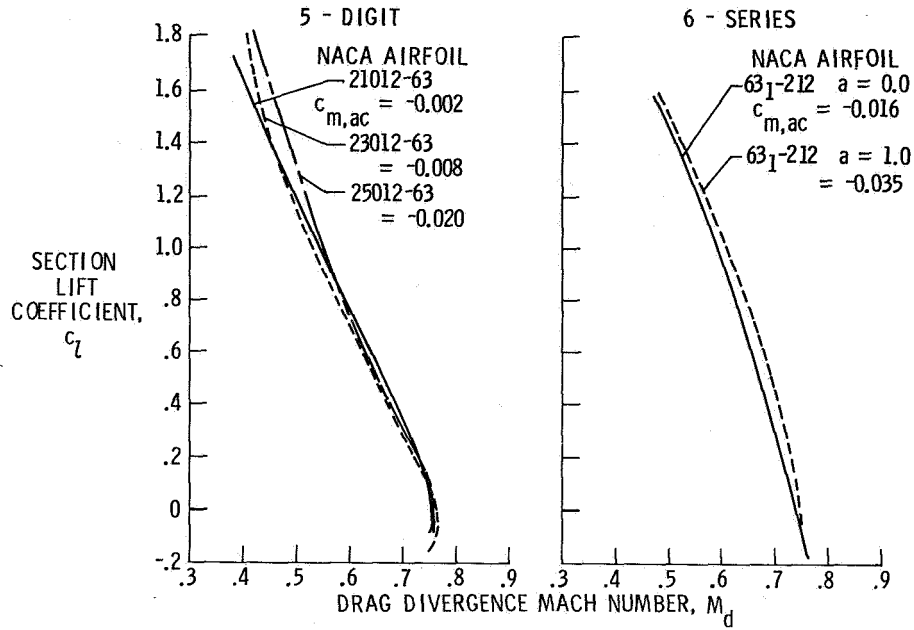


Figure 8.- Influence of position of maximum camber on variation of section lift coefficient with drag divergence Mach number.

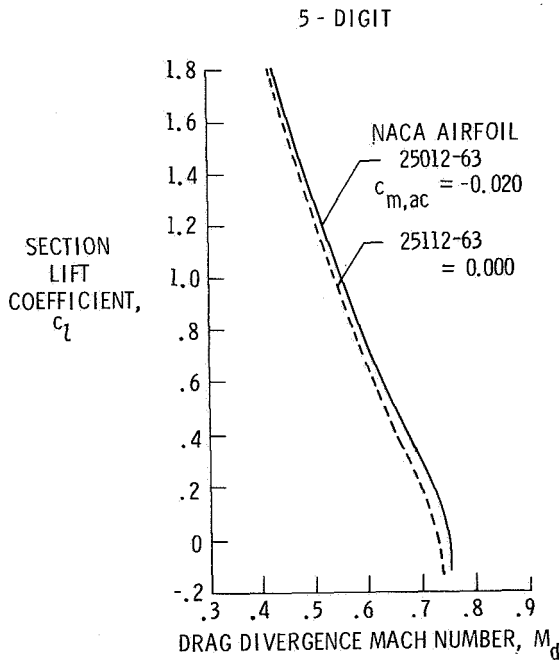


Figure 9.- Influence of reflex camber on variation of section lift coefficient with drag divergence Mach number.

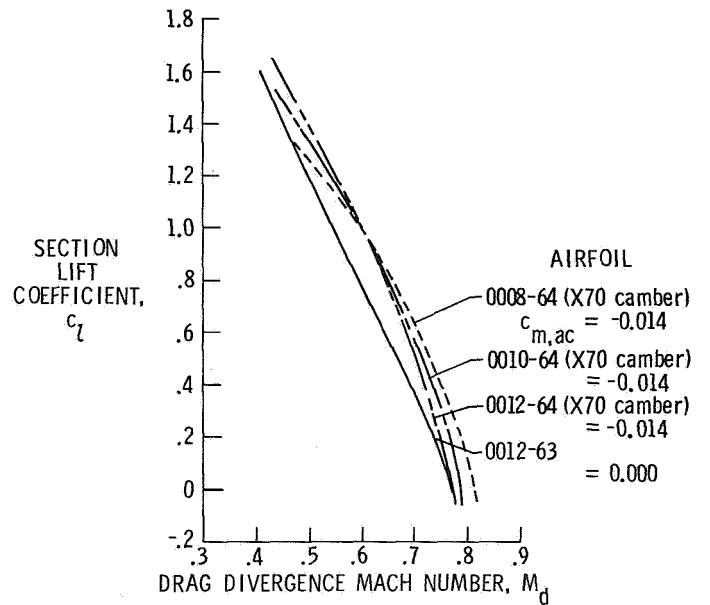


Figure 10.- Influence of combination of geometric parameters on variation of section lift coefficient with drag divergence Mach number.



POSTMASTER: If Undeliverable (Section 158  
Postal Manual) Do Not Return

*"The aeronautical and space activities of the United States shall be conducted so as to contribute . . . to the expansion of human knowledge of phenomena in the atmosphere and space. The Administration shall provide for the widest practicable and appropriate dissemination of information concerning its activities and the results thereof."*

—NATIONAL AERONAUTICS AND SPACE ACT OF 1958

## NASA SCIENTIFIC AND TECHNICAL PUBLICATIONS

**TECHNICAL REPORTS:** Scientific and technical information considered important, complete, and a lasting contribution to existing knowledge.

**TECHNICAL NOTES:** Information less broad in scope but nevertheless of importance as a contribution to existing knowledge.

**TECHNICAL MEMORANDUMS:** Information receiving limited distribution because of preliminary data, security classification, or other reasons. Also includes conference proceedings with either limited or unlimited distribution.

**CONTRACTOR REPORTS:** Scientific and technical information generated under a NASA contract or grant and considered an important contribution to existing knowledge.

**TECHNICAL TRANSLATIONS:** Information published in a foreign language considered to merit NASA distribution in English.

**SPECIAL PUBLICATIONS:** Information derived from or of value to NASA activities. Publications include final reports of major projects, monographs, data compilations, handbooks, sourcebooks, and special bibliographies.

**TECHNOLOGY UTILIZATION PUBLICATIONS:** Information on technology used by NASA that may be of particular interest in commercial and other non-aerospace applications. Publications include Tech Briefs, Technology Utilization Reports and Technology Surveys.

Details on the availability of these publications may be obtained from:

SCIENTIFIC AND TECHNICAL INFORMATION OFFICE

NATIONAL AERONAUTICS AND SPACE ADMINISTRATION

Washington, D.C. 20546